ABSTRACT

Modeling Canopy Foliar Traits and Disturbance Interactions in Central Texas Woodlands

Jonathan A. Thomas, M.S.

Mentor: Joseph D. White, Ph.D.

The present study examines canopy foliar traits and their interactions with the greater ecosystem at multiple scales. Leaf mass/area ratios, nitrogen, and phosphorus were measured and were shown to correlate with relative light levels in some species. Leaf nutrition is used as the basis for a leaf development model. Leaf mass and leaf area index data are utilized to calculate canopy fuels. Species presence/absence at sites is shown to result in significantly different crown fuel loadings. A multiple linear regression approach was adopted to create mapping that takes into account crown bulk density (CBD) spatial heterogeneity. This mapping was used for a series of crown fire simulation comparisons. Fire simulation data show significantly greater frequency of active crown fire occurrence with modeled CBD mapping. Active crown fire initiation is shown to be a function of fuel contiguity levels not achieved by average CBD mapping.

Modeling Canopy Foliar Traits And Disturbance Interactions In Central Texas Woodlands

by

Jonathan A. Thomas, B.S.

A Thesis

Approved by the Department of Biology

_____

Robert D. Doyle, Ph.D., Chairperson

Submitted to the Graduate Faculty of
Baylor University in Partial Fulfillment of the
Requirements for the Degree
of
Master of Science

Approved by the Thesis Committee

_____

Joseph D. White, Ph.D., Chairperson

_____

Ryan S. King, Ph.D.

_____

Steve I. Dworkin, Ph.D.

Accepted by the Graduate School
May 2009

_____

J. Larry Lyon, Ph.D., Dean

Page bearing signatures is kept on file in the Graduate School.

TABLE OF CONTENTS

LIST OF FIGURES

LIST OF TABLES

ACKNOWLEDGMENTS

I would like to acknowledge my mentor and friend, Dr. Joseph White for his patience, diligence, knowledge, expertise, and wisdom in the planning, execution, and completion of this research. I would like to thank the other members of my committee, Dr. Steve Dworkin, and Dr. Ryan King for their technical assistance, scientific advice, and material assistance with all stages of this project.

I would also like to thank my many field assistants, Joanna Thomas, Samir Moussa, Jeff Mink, Dr. Shannon Hill, Bruno Fontes, Karen Ridenour, and Landon Temple. I would further like to thank the land managers in my study area for their field assistance, expertise, and time: Dr. Chuck Sexton, Deborah Holley, and Carl Schwope of the BCNWR, and Glen Gillman of the City of Austin, Water Department. For their laboratory assistance I would like to thank Jeff Back and Dr. Thad Scott. For their myriad forms of assistance and moral support, I would like to thank my labmates, Darrel Murray, Mary Sides, and Yao Jian.

I would also like to thank my family and friends, especially my patient and lovely wife, for putting up with my distance, both physical and emotional, throughout this process.

I would also like to acknowledge those agencies whose funding made this research possible: the United States Geographical Survey and the City of Austin.

CHAPTER ONE

Introduction

Significance of this Study

The woodlands of the BCNWR are a complex mixture of woody species with different life history traits, drought tolerances, and importance to wildlife. This study is designed to describe aspects important to the ecology of the BCNWR woodlands. Canopy characteristics that affect production in dominant species of the woodlands will be analyzed as a step towards improved growth efficiency modeling (Monteith 1977). Leaf mass/area (LMA) ratios are examined to defined species-based differences in LMA. These differences are compared statistically to determine if life history traits such as leaf longevity effect LMA patterns in these woodlands. LMA is further correlated to changes in light transmissivity along vertical gradients in tree canopies.

Leaf nutrition is further explored in this study. Leaf N and P averages are examined for differences among species and the relationship between leaf nutrition and life history traits such as leaf longevity, light tolerance, and edaphic nutrient recycling rates. Leaf N and P are also correlated to incident light transmittance. The importance of species-based leaf morphology characteristics in modifying relationships between foliar nutrients and light is also examined.

Canopy structural traits, including calculation of crown mass (CM), crown bulk density (CBD), and total aerial fuels (TAF) was carried out in this study. These data were compared for differences between the two refuge areas examined in this study. Data were assessed on a 1-m vertical scale and these 1-m layer data were used to

compared canopy mass averages between species. CBD and TAF values were compared between sites for differences related to topography and species presence/absence. LANDSAT 7 ETM+ data were then used to develop a simple linear model for mapping CBD across spatial gradients based on planetary reflectance. This approach did not result in a successful model, therefore a multiple linear regression model was devised, utilizing 3 spectral bands from 2 seasonally different images, and topographic data. This regression equation was used to map CBD across the two refuges in the study area.

CBD mapping produced in this study was used to test hypotheses concerning spatial heterogeneity of crown fuels and associated fire behavior. Fire behavior simulations were carried out using FARSITE (Finney, 1994). Fires were modeled with spatially heterogeneous CBD layers and then duplicated using a spatially homogeneous CBD layer that conferred average maximum 1-m CBD value from this study on the entire landscape. Crown fires were compared for area, intensity, and spread rate on the basis of crown fuel heterogeneity or homogeneity. Fire extent and crown fire extent were also compared between the two refuges in the study area. Fire season variables were also compared as simulations were carried out under summer and winter weather scenarios. Crown fuel values associated with active crown fire events in simulations were examined as active crowning fire only occurred in heterogeneous crown fuels mapping scenarios.

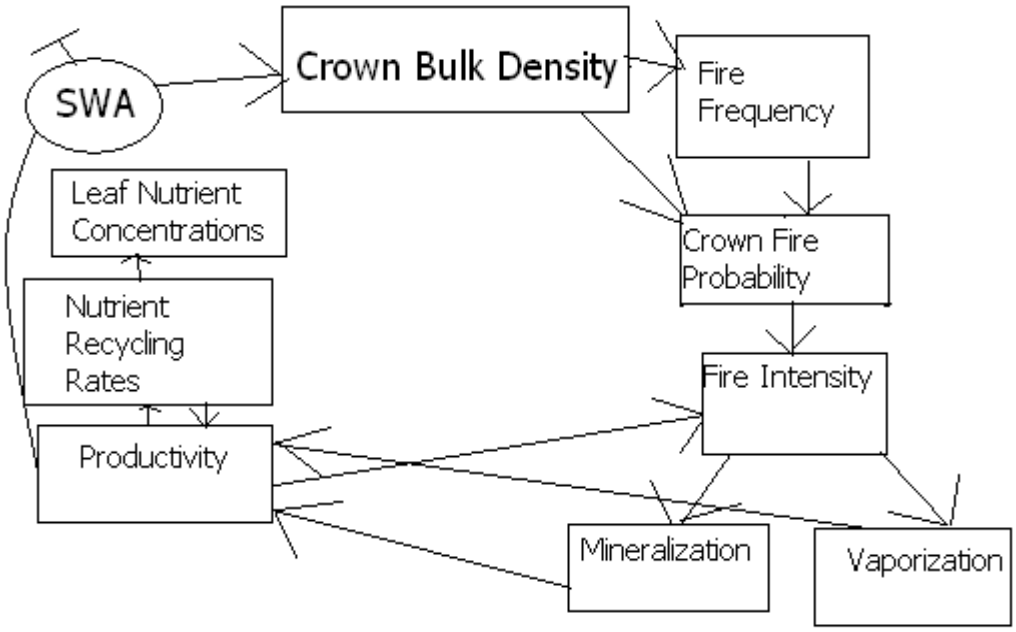

Figure 1. Conceptual model of research indicating system feedbacks between leaf morphology, nutrition, growth rates, disturbance, and topography. Soil water availability (SWA) accounts for topographic and gross edaphic variation.

The above conceptual model indicates the feedbacks between leaf characteristics, stand level dynamics, and landscape level disturbance. Elaborating current knowledge of woodland canopies in the study area at multiple scales is therefore important to land management and fire risk assessment in these lands. Specifically, the following general questions are addressed by the hypotheses presented within this work:

Is leaf morphology related to species' life history traits?

Do leaf mass/area ratios quantifiably relate to intercepted light intensity?

Are leaf nutrient levels related to intercepted light intensity?

Does leaf nutrient stoichiometry modulate a species' local edaphic environment?

Do crown fuel magnitudes differ among tree species?

Is stand level crown fuel related to species presence/absence?

Does planetary reflectance data reliably predict crown fuel magnitude?

Do spatially heterogeneous crown fuels affect crown fire behavior?

Do seasonal differences in meteorology affect fire impact outcomes?

Site Description

The Balcones Canyonlands National Wildlife Refuge (BCNWR) (Lat30.32N, Long. 97.73W) and Balcones Canyonlands Preserve (BCP) (Lat. 30.63N, Long. 98.04W) are located in the central Texas hill country of the Edwards Plateau Region. BCNWR is a U.S. Fish and Wildlife Service (USFWS)-owned area that is comprised of 6,500 ha within an acquisition boundary of approximately 18,600 ha. BCP lands are comprised of 5,300 ha within an acquisition boundary of 12,315 ha. The BCP lands are owned and managed jointly by the City of Austin, Texas and Travis County, Texas. Both of these preserves are comprised of a system of land tracts which are actively managed for endangered species and species of concern. These refuge lands are interspersed with private lands, primarily comprised of grazing operations for BCNWR, and urban development for BCP. The refuges serve as breeding grounds for two federally listed endangered species of birds: the golden-cheeked warbler (*Dendroica chrysoparia*), and the black-capped vireo (*Vireo atricapilla*) (USFWS, 1992). The geology of the Balcones region is marked by the Glen Rose (upper Cretaceous), Walnut (lower Cretaceous), and Edwards (lower Cretaceous) limestone formations. The area is covered by well-drained, clay loam soils, and traverses over 300 m of relief. The clay-rich limestone of the Walnut formation drives the water-balance of the area as it induces lateral sheet flow of moisture, unlike the high-porosity of the overlying Edwards formation. The valley areas of the

refuge are dominated by grasslands comprised of *Andropogon gerardii*, *Bouteloa gracilis*, *Schizacyrium scoparium*, and the introduced invasive *Bothriochloa ischaemum*. Creek bottoms are covered by a number of tree species including: *Carya illinoiensis*, *Juglans nigra*, *J. major, Ulmus crassifolia*, *Melia azedarach*, *Populus deltoides*, *Prunus serotina*, *Quercus buckleyi*, *Juniperus ashei*, and *Q. fusiformis*. The mid-slope regions are dominated by *J. ashei* and *Q. fusiformis* at most aspects, though north-facing slopes tend be dominated by the deciduous oaks *Q. buckleyi* and *Q. sinuata,* as well as a number of sub-dominant deciduous species including *P. serotina*, *Diospyros texana*, and *U. crassifolia*. The hilltops are frequently composed of short, scrubby *J. ashei* thickets (colloquially known as cedar brakes), grasslands (with same species as valleys), *Opuntia* thickets, bare limestone or shrubby *Q. sinuata* stands. These *Q. sinuata* stands, known as shinneries, grow to only around 4m as the Edwards formation derived soils are shallow and have very little capacity to hold water.

Four tree species were examined in this study and dominate much of the woodlands of this area. The four tree species studied were: *J. ashei*, *Q. fusiformis*, *Q. buckleyi*, and *Q. sinuata*. *J. ashei* is a scaled-leaf evergreeen conifer that grows to around 8m and predominates on drier soils, is probably shade intolerant (Sullivan, 1993), does not resprout, and is dispersed by large crops of berries by mammals and birds. *Q. fusiformis* is an evergreen broad-leaved oak that can grow 10m, prefers dry slopes, is medium in shade tolerance (Carey, 1992), vigorously resprouts post-fire, and is primarily dispersed via lateral root-sprouting. *Q. buckleyi* is a decidous, broad-leaved oak that grows to around 12m, is shade intolerant (Sullivan, 1993), prefers well-watered, loamy soils and resprouts vigorously from the root ball. *Q. sinuata* is a deciduous, broad-leaved

oak that is shade and competition intolerant (Carey, 1992) and grows to around 10m in deeper soils and can grow in shrubby forms to less than 4m (known as shinneries) in shallow soils. It prefers wetter, loamy soils and actively sprouts from the root ball in a crown formation post-disturbance.

CHAPTER TWO

LMA, Leaf Nitrogen and Phosphorus per Unit Area Varies with Light Transmissivity in Selected Central Texas Tree Species with Different Leaf Longevities

Abstract

Leaf mass per unit area (LMA), foliar nitrogen and phosphorus concentrations and light transmissivity were measured at various depths in the canopies of four tree species in Central Texas to assess mass and nutrient allocation strategies. Species selected included a scale-leafed evergreen *Juniperus ashei*, a broad-leafed evergreen *Quercus fusiformis*, and two deciduous broad-leafed species *Q. buckleyi* and *Q. sinuata*. Results showed that LMA significantly increased with transmissivity in *J. ashei*, *Q. buckelyi*, and *Q. sinuata*. Linear regression modeling indicated that the slopes of these three species were statistically similar indicating a uniform response to canopy light intensity. Leaf nitrogen per unit area (N/area) increased significantly with transmissivity in *Q. buckleyi*, *Q. fusiformis*, and *Q. sinuata*. Slopes were statistically similar in *Q. buckleyi* and *Q. fusiformis*. Leaf phosphorus per unit area (P/area) was also significantly correlated with transmissivity for *Q. buckleyi* and *Q. sinuata*. C:N ratios were significantly higher in evergreen leaves and N:P ratios significantly higher in oak species than the conifer species sampled. Results indicate evolutionarily conservative leaf mass developmental mechanisms and species-specific adaptive interactions to leaf litter nutrient stoichiometry.

Introduction

Foliar traits in trees, such as leaf morphology, nutrient allocation, and leaf longevity, are related due to the inherent trade-off between longevity and productivity (Reich, et. al, 1992). Leaf morphology is an important competitive factor among co-occurring tree species as leaf area/mass relationships affected intercepted light (Ellsworth and Reich, 1996; White and Scott, 2006). The proportion of light that filters through a canopy to a given position, or transmissivity (τ), interacts positively with leaf mass to area ratio (LMA) consistently across different species (Ellsworth and Reich, 1996, Meir et. al, 2001; White and Scott, 2006). The LMA of foliage in the canopy is also strongly related to leaf nitrogen concentration on an area basis (N/area) (Ellsworth and Reich, 1993). Also leaves have previously been shown to decrease productivity levels with age, particularly on a mass basis (Reich, et. al, 1992).

Canopy photosynthetic carbon gains are related both to LMA and canopy nutrient distribution. Based on CO_2 capture, light use efficiency (LUE) is inversely related to LMA by a curvilinear function and nitrogen per unit mass (%N) has been shown to correlate linearly to LUE (Green et. al, 2003). Kazda, et. al (2000) showed that leaves sampled from different species showed similar photosynthetic nitrogen use efficiencies (PNUE) at light saturation at the same canopy position (height). These relationships indicate that species show strong responses to ambient light environment and that competition drives species to achieve similar levels of photosynthetic efficiency with regards to both light and nutrients when integrated over space and time. However, phylogenetic traits such as leaf longevity moderate this response as demonstrated by Takashima, et al (2004) who showed that different N/area values existed between

congeneric oak species and that this difference was largely based on the consequences of differences in leaf longevity. Phosphorus is also related to the photosynthetic machinery of the plant canopies as ATP in the cells is expected to increase with light transmission (Harley et al. 1992). These relationships imply that within any given environment, tree species composition is affected by differences in leaf longevity and associated with leaf morphology and nutrient concentration gradients.

Leaf longevity potentially moderates nutrient cycling with ecosystem feedbacks on foliar nutrient concentration (Pastor and Post, 1986). The nutrient content of foliar litter controls site N availability where nitrogen mineralization is limited. The C:N ratios of 35:1 in bacteria-dominated and 10:1 in fungi-dominate soil environments were found to be in equilibrium with regard to N mineralization and immobilization (Austin et al, 2004). Pastor, et al (1984) showed that N mineralization rates correlated strongly to total P in leaf litter. This same study also showed a strong negative correlation between C:P ratios and N mineralization rate. Phosphorus availability has also been shown to relate directly to rapid pulses of soil water associated partially with microbial cell lysis due to osmotic shock. (Turner and Haygarth, 2001). Together, these findings suggest an understanding of the relationships between leaf longevity and nutrient concentration is important to an understanding of overall site nutrient balance.

In the current study, we demonstrate that LMA differs among selected Central Texas tree species as a function of leaf longevity. Nutrient concentrations, such as nitrogen and phosphorus, also differ among species and both leaf N and P per unit area increases linearly with light transmissivity. Finally, mean values of C:N and N:P ratios

also differ significantly among the species analyzed on the basis of leaf longevity. Evergreen species have higher mean C:N ratios while deciduous trees have higher N:P.

Materials and Methods

Field Canopy Sampling

As light is intercepted by leaves in a canopy, photons are either reflected back into the atmosphere, absorbed or are transmitted through the canopy to the underlying layers of leaves. The transmissivity (τ) of a plant canopy is described by the Beer-Lambert equation:

$$\tau = \exp^{(-k*LAI)} \qquad \text{eq. 1}$$

where LAI is leaf area index, and k is an extinction coefficient. The LAI-2000 Plant Canopy Analyzer (Li-Cor, Lincoln, NE) calculates this light attenuation based on brightness measures at five zenith angles simultaneously and compares those to readings taken outside the canopy:

$$LAI = \Sigma\{[-\ln(\varphi_{in}/\varphi_{out})]s\} \qquad \text{eq. 2}$$

Where φ is the radiant flux, and s is the average distance to the vegetation at each of the zenith angles. For this study, the LAI-2000 was utilized to estimate LAI at multiple levels in canopies and to derive extinction coefficient values to derive τ (Vose, et al, 1995).

Sample sites were chosen in stratified random sampling manner were at least 50 m apart, and had the highest possible diversity in tree species. Measurement of canopy gap fraction with the LAI-2000 were taken from the tops of tree canopies to the ground level at 1 m intervals using an extendable pole between May-July, 2007. Transmissivity

(τ), at each 1 m level within the canopy to that measured outside (above) the canopy derived from the LAI-2000 data. Leaf samples, approximately 5 to 15 leaves, were also collected at each of these height intervals with a branch pole pruner. These were stored and refrigerated in air tight plastic bags to retain leaf moisture and promptly returned to the laboratory for analysis.

Laboratory Analysis

Collected leaf samples were measured for projected leaf area with a flatbed digital scanner (Microtek Lab, Fontana, California) and analyzed to convert pixel area to cm^2 with Adobe Photoshop (Adobe Systems Incorporated, San Jose, California). Planar leaves (those of the broad-leaved species) had projected areas doubled to account for both upper and lower surfaces in the LMA calculation. Cylindrical leaves (those of needle-leaved species) had projected area values multiplied by π to approximate total surface area for exposed leaf surfaces (Grace 1983). These leaves were then dried at 60°C for 48 hours and weighed to 0.01 grams. Total leaf dry mass was divided by calculated leaf area for each sample to compute LMA. These values were recorded for each sample, from each species, at each site and canopy position.

The leaves that were utilized for LMA measurements were ground in a bead beater (Bio-Spec, Tulsa, OK) to uniform consistency. The ground leaf matter was processed for N and C content in a Flash Elemental Analyzer 1112 (CE Industries, UK). This instrument operates via thermocombustion and gas detection measures compared to calibration curves created from samples of known concentrations. Phosphorus concentrations were measured by a combined acid digestion and colorimetric analysis. Powdered leaf sample was digested in a 5 ml sulfuric acid bath with one Kjeltab

(Thompson and Capper LTD, UK) containing 1.5 g K_2SO_4 and 0.5 g Cu SO_4 with 2 boiling chips. The bath consists of ramping the temperature to 250°C and holding for 30 minutes, then ramping to 350°C and holding for 120 minutes. This is controlled by an AIM 500 Programmable Controller (A.I. Scientific, Australia). The acid-digested samples were resuspended and cooled for at least four hours before dilution to 75 ml. Dilute samples were then analyzed for total phosphorus content with the Lachat system (Lachat Instruments, Milwaukee, WI). This system operates by colorimetric detection of reactive species after molybdate and ascorbic acid reactions occur within liquid samples.

Calibration curves were difficult to generate and standard concentration test samples deviated from these curves over time. This error is assumed to be related to detection of the complex matrix generated by the extraction methods.

Analysis

All data were analyzed in SPSS 13.0 (SPSS Inc., Chicago, IL). All parameters tested were considered normally distributed based on the results of Kolmogorov-Smirnov analyses, where asymptotic 2-tailed significance values of >0.95 were considered normal. Comparison of measured LMA on the basis of species was achieved utilizing Tukey's B to compare parameter magnitude for significant differences (α-level set to 0.05). The data were then randomly place in sub-sets by selecting one sample from each tree. This was done to avoid the effects of pseudo-replication in subsequent analyses. These samples were correlated to their corresponding τ values and examined for significance based on least-squares regression analysis. Regressions were measured for significance by setting α=0.05. Regressions equations were compated by the methods of Kleinbaum et. al (1988).

Leaf nutrient concentrations were converted to a per area basis by multiplying percent mass nutrient concentrations by LMA values for each sample. Also, the mean values by species were statistically examined to detect differences in mean on a species basis as with the analysis of LMA. The same randomly selected samples as above were used in regression analysis with respect to τ and analyzed in the same manner. Stoichiometric ratios were calculated then compared using the same listwise comparison method used above. Regression analyses were carried out with stoichiometric values, though no significant relationships were evident.

Results

Leaf attributes are compiled in Table 1. Highest mean LMA values are seen in the leaves of *J. ashei* and lowest in the leave of the deciduous oak *Q. buckleyi*. Generally, data show higher mean LMA values for the evergreen species. All species show %C values near 0.50. Mean leaf nitrogen content values are highest in *Q. sinuata* leaves at 2.01% and lowest in *J. ashei* at 0.82%. N/area values are highest in *Q. fusiformis* at 1.04 g/m^2 and lowest in *J. ashei* at 0.67 g/m^2. Mean leaf phosphorus content values are highest in *Q. buckelyi* at 0.23% and lowest in *Q. fusiformis* at 0.198%. P/area values are highest in *J. ashei* at 0.18 g/m^2 and lowest in *Q. buckleyi* at 0.09 g/m^2. Nutrient concentration values are generally highest for species that are deciduous. C:N ratio values are highest in *J. ashei* at 74.0 and lowest in *Q. sinuata* at 30.9. C:P ratio values are highest in *Q. fusiformis* at 748.3 and lowest in *Q. sinuata* at 628.8. N/P values are highest in *Q. sinuata* at 21.41 and lowest in *J. ashei* at 9.4. C:N ratios are highest for evergreen species while N:P ratios are higher for deciduous species.

Statistically significant differences are ranked among the four major species of this study in Table 2. Significant differences exist between species with respect to LMA.

Table 1. Summary data for all sampled leaves. Values given are mean plus/minus standard deviations where LMA indicates leaf mass per unit area, %C is percent carbon by mass, C/area is carbon mass per unit area, %N is percent nitrogen by mass, N/area is nitrogen per unit area, %P is phosphorus per unit mass, P/area is phosphorus per unit area, and C/N, C/P, and N/P area stoichiometric ratios in moles over moles.

Species	*J.ashei*	*Q. fusiformis*	*Q. buckleyi*	*Q. sinuata*
Trees sampled	31	23	39	19
Leaves sampled (n)	169	140	257	115
LMA (g/m^2)	83.1± 11.1	73.6± 11.7	38.7± 7.3	47.2± 11.4
%C	50.14± 3.705	49.80± 3.860	50.80± 3.681	50.53± 4.719
C/area (g/m^2)	41.53± 6.30	36.33± 6.03	20.01± 4.01	24.16± 5.79
%N	0.815± 0.163	1.436± 0.317	1.845± 0.321	2.012± 0.485
N/area(g/m^2)	0.671± 0.147	1.039± 0.264	0.734± 0.175	0.941± 0.247
%P	0.212± 0.066	0.198± 0.065	0.232± 0.073	0.226± 0.063
P/area (g/m^2)	0.177+- .062	.0144± 0.050	0.092± 0.032	0.105± 0.033
C:N	74.02± 12.49	42.09± 8.79	32.75± 7.53	30.94± 8.03
C:P	683.7± 262.1	748.3± 336.2	636.5± 267.8	628.8± 215.9
N:P	9.35± 3.87	18.73± 10.19	20.09± 8.94	21.41± 8.39

Table 2. Ranking of means for each of 4 major species analyzed. Numbers indicate rankings of parameters based on pairwise comparison (Tukey's HSD) carried out with α=.05. Data indicated significant differences exist among species measured for all parameters with exception of %C, %P, and C:P. Where two rank numbers are listed, pairwise comparison showed significant similarity to two other species that were themselves not statistically significant.

Species	LMA	%C	%N	N_{area}	%P	P_{area}	C:N	C:P	N:P
J. ashei	1	-	3	2	-	1	1	-	2
Q. buckleyi	3	-	1	2	-	3	3	-	1
Q. fusiformis	2	-	2	1	-	2	2	-	1
Q. sinuata	3	-	1	1	-	2,3	3	-	1

J. ashei leaves have the highest values of LMA, followed by *Q. fusiformis*, *Q. sinuata*, then *Q. buckleyi*. These rankings are all significantly different (α<0.05). *J. ashei* and *Q. buckleyi* leaves exhibited the lowest levels of N/area while *Q. fusiformis* and *Q. sinuata* were higher. The two deciduous tree species (*Q. sinuata* and *Q. buckleyi*) also had the highest %N, followed by *Q. fusiformis*, which was higher than *J. ashei*. *J. ashei* leaves had the highest P/area, differing from the next highest *Q. fusiformis*, which was statistically different from *Q. sinuata* and *Q. buckleyi*. *J. ashei* leaves had the highest significantly different C:N ratio, followed by *Q. fusiformis*, which was significantly greater than C:N ratios for the statistically equivalent C:N ratio values for *Q. sinuata* and *Q. buckleyi*. C:P ratios were not statistically different. The three *Quercus* spp. analyzed exhibited statistically higher N:P ratios values than *J. ashei*.

Figure 2 illustrates that LMA correlates significantly to τ values. Three of the four major species sampled showed positive linear correlations to τ. This relationship was significant for two deciduous oak species (*Q. buckleyi* and *Q. sinuata*) and an

evergreen conifer (*J. ashei*) sampled here. Comparison of slopes by the method of (Kleinbaum et al., 1988) was used in pairwise fashion to test a null hypothesis that regression slopes did not differ significantly at α=.05.

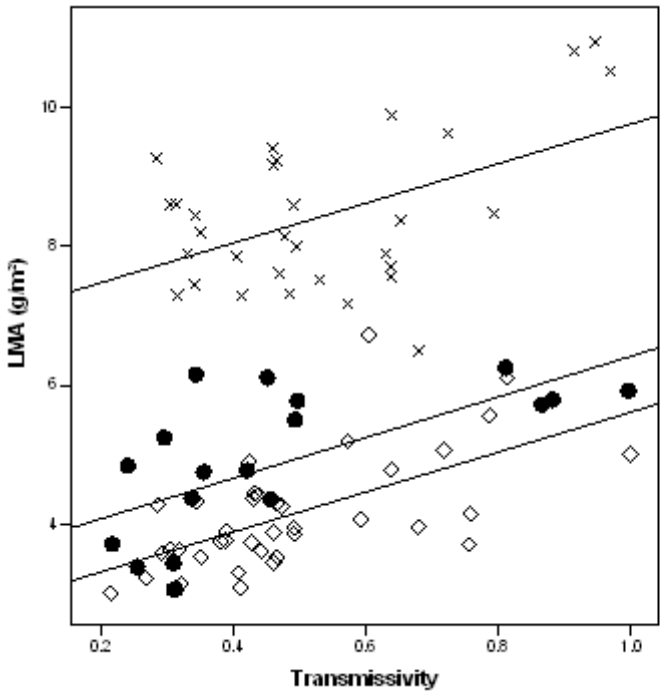

Figure 2. Leaf mass to unit area for leaves are shown to correlate linearly with light transmissivity values. Correlation of LMA with light transmissivity was highest for *Q. sinuata* (darkened circles) (r^2=.408, p=.003), followed by *Q. buckleyi* (◊) (r^2=.381, p<.001), and then *J. ashei* (×) (r^2=0.24, p=.005). *Q. fusiformis* leaves did not show a significant relationship. Species regression slopes did not significantly differ (p<.001).

Figure 3 illustrates that N/area correlates signficantly to τ values. This relationship was significant for two deciduous oak species (*Q. buckelyi* and *Q. sinuata*), and an evergreen oak species (*Q. fusiformis*) sampled here. Comparison of slopes for parallelism showed that *Q. buckleyi* and *Q. fusiformis* had statistically similar regression slopes (p=.262) in a test of the null hypothesis of slope parallelism. The regression slope of *Q. sinuata* was significantly different from that of both *Q. buckleyi* (p<.001) and *Q.*

fusiformis (p<.001). N/area response to light does not appear to be conserved across all species.

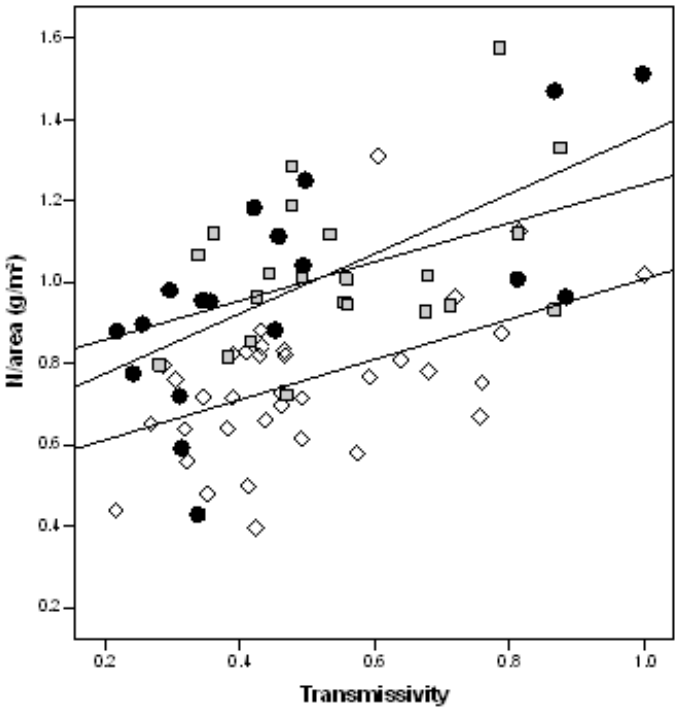

Figure 3. Nitrogen per unit area for leaves are shown to correlate linearly to light transmissivity values. Correlation of N/area to light was highest for *Q. sinuata* (darkened circles) (r^2=0.44, p=.003), followed by *Q. buckleyi* (◊) (r^2=0.23, p=.003), then *Q. fusiformis* (shaded boxes) (r^2=.19, p=.040).

Figure 4 shows that P/area correlates significantly to τ values. This relationship was significant in two of the major species sampled, both deciduous oaks (*Q. buckleyi* and *Q. sinuata*). The slopes of the two regression lines shown here do differ significantly in slope (p<.001). P/area response to light does not appear to be conserved across species.

Discussion

Leaf Morphology

The data in Table 1 indicate increased LMA among evergreen species versus deciduous species. These differences are significant among the four major species sampled (Table 2). Mechanistically, this implies that leaf age plays a role in leaf mass development after expansion is complete. From an evolutionary perspective, it is also likely that evergreens do not tend to expand as much as congeneric deciduous species due to decreased requirements for light competition. A decreased necessity for light competition is explained by wintertime photosynthetic activity for *J. ashei*.

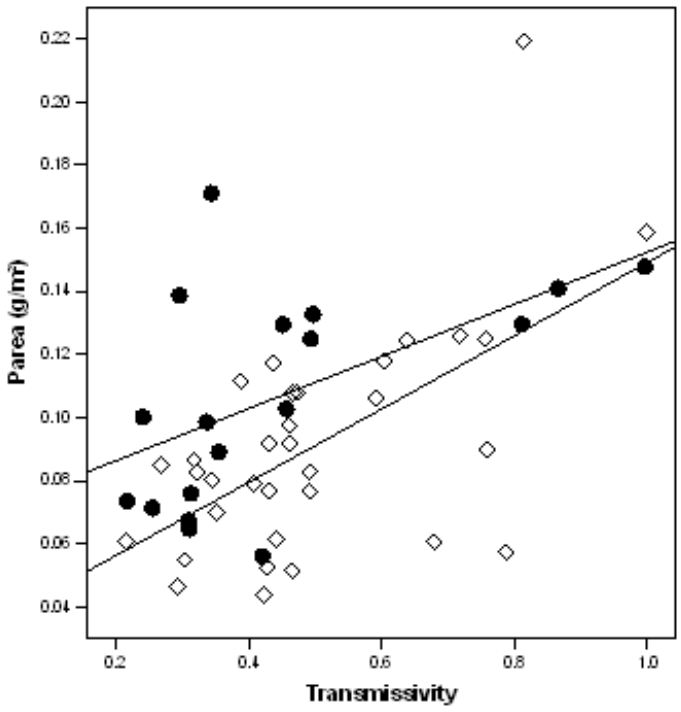

Figure 4. Phosphorus per unit area for leaves area shown to correlate linearly to light transmissivity values. P/area to light correlation was highest for *Q. buckleyi* (◊) (r^2=0.35, p<.001), followed by *Q. sinuata* (darkened circles) (r^2=0.30, p=.019).

This study confirms that LMA changes with τ and that this change is relatively uniform amongst the species. This finding represents quantified evidence that transmitted light affects leaf mass/area ratios. Leaf morphology changes with respect to canopy position (Ellsworth and Reich 1993, Meir et al. 2001, Green et al. 2003) partially as a function of intercepted light (White and Scott, 2006). The species response to light is also fairly uniform based on the result of the slopes of the regression between light transmissivity and LMA that were statistically similar ($p<0.001$) for three of the four species including the deciduous broadleafed *Quercus* spp. and evergreen scaled conifer (*J. ashei*). This result, coupled with similar results in other ecosystems in previous studies (Hollinger, 1989, Griffin et al, 2001, White and Scott, 2005) strongly suggests an evolutionarily conserved mechanism for LMA development across terrestrial vegetation types. Species independent responses have also been identified (Ellsworth and Reich, 1996) inferring some uniform underlying process for leaf development under different irradiances.

Leaf breadth and length are established both allometrically based on the species and through overall water limitations associated with soil water potential (Myers 1988). The concept of viewing leaves as a set of layers that thicken in the presence of intense light is valid, but only provides a partial explanation. Leaf expansion may also be affected by high transmissivity due to water stress associated with transpiration. Previous studies have indicated that lack of leaf expansion due to water stress over the growing season explains lowered LMA among needle-leaved conifers (Myers, 1988, Specht and Specht, 1989) and the results presented here corroborate this mechanism, though based

on the low coefficients of determination in the regressions between τ and LMA, other factors likely contribute to the development of LMA.

Nutrient Concentration

Nutrient allocation patterns of species with different leaf longevities differ in this study. Evergreen species tended to have lower nutrient concentrations on a mass basis but higher per unit area (Tables 1 and 2). This is explained by greater LMA values for evergreens (Table 2). Leaf area appears to play a role in increasing nutrient concentrations per unit mass. This may involve a mechanism where transpiration is the source of nutrients from roots and greater sap flux results in higher nutrient concentrations at leaves in different parts of the canopy.

N/area values increased linearly across a radiation gradient for three species in this study: *Q. fusiformis*, *Q. buckleyi*, and *Q. sinuata*. *Q. fusiformis* did not show such a relationship for LMA values indicating that N allocation is related in this species directly to light, not LMA changes. Different regression slopes in N/area-transmissivity regressions in this study argues for a species-based (possibly genetic) difference in N allocation patterns. Such independent responses in foliar N have been show in a previous study (White and Scott, 2005).

Based on the different slopes of P/area to τ found in the two deciduous oak species analyzed in this study, P allocation is species-specific influenced by metabolic demands within each tree. Mean P/area values were associated with leaf longevity in this study. Greater P/area allocation in evergreens is likely a function of greater LMA.

These results also imply that leaf water balance is also related to the foliar nutrient values as a function of irradiance. Greater leaf area is an adjustment to lower τ levels.

This may serve to not only enhance light capture, but also to allow enough transpiration to accumulate nutrients. Assuming the sap has a fairly uniform concentration of nutrients (e.g. N, P) a constant canopy foliar nutrient concentration (nutrient/mass) is associated with the leaf transipiration. As leaf size is modified by leaf water, coupled with lower leaf water potentials (Myers 1998) with higher irradiance, transpiration per leaf area may also be constant throughout the canopy. The deposition of nutrients is indirect due to transpiration and water balance stream with water transpired, termed here hydraulic serendipity. Changes in N/area become mostly a function of LMA (Niinemets 1999) coupled with balance by diffusion between the sap and foliar water nutrient concentrations. However, *Q. fusiformis* showed no significant correlation between transmissivity and LMA (Figure 1), but did show a significant relationship between transmissivity and N/area (Figure 2). One possible explanation is that leaves in this study were collected within four months of emergence. Live oaks leaves are extremely sclerophyllous compared to the other species in this study (Monk 1987) which develops over several months. First, mass accumulation occurs due to other factors besides at-leaf irradiance. Second, maximum nitrogen accumulation occurs asynchronously with maximum leaf mass and area formation. Also, N is retranslocated frequently in some species as nitrogenous compounds are partitioned to leaves to supply optimal protein (e.g. RuBisCO) demand for photosynthesis. Whether this reallocation is directed by genetic mechanisms or by transpiration streams is presented here as a topic for future analysis.

Stoichiometry

Stoichiometry of leaf matter may affect changes in nutrient recycle rates if retranslocation is either non-selective or insignificant. Elevated C:N ratios in evergreen

trees may represent nutrient cycling rate strategies that can be advantageous to these species. Evergreen species examined above (Table 1) show significantly higher C:N ratios than deciduous species sampled, with *J. ashei* ranking highest, followed by *Q. fusiformis*, then the two deciduous oak species. Discounting the possibility of highly specific nutrient re-translocation, such an elevation of C:N ratio can serve to decrease nutrient recycle rates (Austin 2004) by sequestering N in bacteria or fungi. As stated above, C:N ratios below 35:1 show net N mineralization to soils. The two deciduous species intensely sampled show mean C:N ratios lower than this threshold while the evergreen oak *Q. fusiformis* and the scaled-leaf evergreen conifer *J. ashei* both showed mean C:N values higher than this threshold, indicating net immobilization in bacterially-dominated soil communities. This result indicates that effects of P in leaf litter likely have little demonstrable effect on N cycling in the system studied. Higher N:P values observed for *J. ashei*, may indicate slower P recycling rates in litter as P becomes limiting for decomposing microbes. The ecophysiological function of this is lower site P availability with a decrease in plant competition. This could both affect productivity due to lack of P and slow N mineralization in leaf litter (Pastor et al, 1984). Species that have short leaf longevities and/or limited capacity for retranslocation would be adversely affected by such slow turnover rates. Furthermore, species such as *J. ashei* would benefit from the microclimate modification of their evergreen nurse trees (Sullivan, 1993) and the concomitant low nutrient availability that would prevent competitors.

Conclusions

Mean leaf LMA, C/N, and P/area differed significantly among species in a manner consistent with leaf longevity patterns. Species with longer-lived foliage

accumulate greater mass and P/area in leaves. Foliar response to light was measurable and differentiated among species in this study. LMA change over a measured light gradient was uniform in 3 of 4 species showing a significant response. N/area also changed linearly over such a gradient in 3 of 4 species. P/area showed the same effect, but only for deciduous species.

Foliar mass and nutrient accumulation were shown to be distributed in plant canopies according to the abiotic influence of light environment, suggesting these accumulations are based primarily in physicochemical, rather than genetic, processes. Differences among species in mean value, minimum value, and regression intercept values are likely to be derived from individual species genetic differences.

Difference in nutrient ratios represents evolutionary adaptations to reduce competition. Lowered availability of soil N and P relative to soil C represents a set of competitive advantages for species with longer-lived leaves that coexist with other species. Ecologically, species that become dominant in the canopy through pioneering or rapid stand development can enhance their future dominance through alteration of site nutrient cycling and availability.

CHAPTER THREE

Characterizing Canopy Fuels on Balcones Canyonlands Preserve and Balcones Canyonlands National Wildlife Refuge

Abstract

Crown fuel parameters were measured at 1m vertical scale on a variety of Central Texas woodland stand types on two different government-operated wildlife refuges. Based on topographic, fire, and, land use history differences between the refuges, crown fuels were found to be significantly heavier on a volumetric and total basis on the lower-lying, urbanized Balcones Canyonlands Preserve. Species were found to have significant differences in mean canopy mass layer values and leaf mass to unit area (LMA) values. Remote sensing possibilities for crown fuel parameters were explored and a multiple linear regression approach adopted.

Introduction

The woodlands of the Balcones Canyonlands Preserve (BCP) and Balcones Canyonlands National Wildlife Refuge (BCNWR) are a complex mixture of woody species with different life history traits, drought tolerances, and importance to wildlife. This study is designed to describe aspects important to the fire ecology of the BCP and BCNWR woodlands. Growth and form of these woodland canopies potentially influences canopy fire spread as the density of the live fuel of the canopy changes due to species composition and disturbance history at the site. Prediction of canopy fuels spatially is an

important step in assessing fire risk of these lands that exist within an ex-urbanized area through fire behavior modeling.

Canopy architecture can have important effects on crown fire risk (Van Wagner, 1977). The parameters used to describe canopy architecture in this study are crown mass, crown bulk density, total aerial fuels, and leaf area index. Crown mass (CM) is defined as the density of any one layer of canopy (in this study a layer is a $1m^3$ average). Crown bulk density (CBD) is the mass of leaf matter per unit volume in forest canopies and is a valuable determinant of the likelihood of torching and crown fire spread rates (Keane, et al, 2005). Total aerial fuels (TAF), defined here as total dry mass of leaf matter in the canopy per area ground layer, can also lend some insight into tree canopy fire behavior and risk (Dickinson, et al, 2007). Leaf area index is the total leaf area in a canopy per area of ground. Using a method (Keane, et al, 2005) modified to capture vertical variations in canopy structure and fuel loading, this study seeks to reliably enhance crown fuel description.

Remotely sensing studies on foliar biomass density are sparse in the literature despite theoretical support (Park and Deering, 1982). Methods involving stand to landscape scale measures of leaf area and published species average mass/area ratios have been used, though these provide only gross estimates and no estimate of spatial heterogeneity. Since crown fire spread prediction is based on either total crown mass (Dickinson, et al, 2007) or mass density (Van Wagner, 1977), spatial heterogeneity may provide important insight into predicting the likelihood and extent of active crown fires. Thus it is important for land management, fire risk assessment, and ecological enhancement to reliably determine crown fuel loadings at finer scales.

Materials and Methods

Sites were selected in a stratified random manner to achieve highest number of species possible per site. At each site, leaf area index (LAI) data were taken by a light interception method utilizing an LAI-2000 Plant Canopy Analyer (Li-Cor, Lincoln, Nebraska). This method utilizes contact frequencies to determine plant surface area through canopies by the formula:

$$LAI = \Sigma\{[-\ln(\varphi_{in}/\varphi_{out})]s\} \qquad \text{eq. 3}$$

Where φ is the radiant flux, and s is the average distance to the vegetation at each of the zenith angles. LAI was measured at 1-m intervals from the top of canopies to the ground by mounting the LAI-2000 on a 10-m telescopic pole. Samples of leaves were also taken at 1-m intervals from the tops of canopies to ground level (where they existed) to measure leaf mass-area ratio (LMA). Leaf samples were stored in plastic bags to maintain surface area. Ocular estimates of relative leaf area were assigned to each species at each 1-m interval.

Samples were retured to the lab to measure LMA. Collected leaf samples were measured for projected leaf area with a flatbed digital scanner (Microtek Lab, Fontana, California) and analyzed to convert pixel area to cm^2 with Adobe Photoshop (Adobe Systems Incorporated, San Jose, California). Planar leaves (those of the broad-leaved species) had projected areas doubled to account for both upper and lower surfaces in the LMA calculation. Cylindrical leaves (those of needle-leaved species) had projected area values multiplied by π to approximate total surface area for exposed leaf surfaces (Grace 1983). These leaves were then dried at 60°C for 48 hours and weighed to 0.01 grams. Total leaf dry mass was divided by calculated leaf area for each sample to compute LMA.

These values were recorded for each sample, from each species, at each site and canopy position.

LAI and LMA data were used to calculate canopy fuel parameters. CBD is given by the equation:

$$CM = LAI*LMA \quad \text{eq. 4}$$

for each canopy layer measured. LAI is allotted to each tree species noted at the site based on the ocular estimates from the field. Max CM is the densest (highest magnitude of CM) layer of each canopy. These layers are then summed to derive TAF:

$$TAF = \Sigma(CM) \quad \text{eq. 5}$$

to give a site TAF. Site CBD is given by:

$$CBD = TAF/Ht. \quad \text{eq. 6}$$

where Ht. is the height of the canopy in meters. Canopy length is the site height minus the CBH where CBH is defined as the height (to the nearest meter) at which increase in measured LAI ceases (measuring from top to bottom). Skewness is a measure of the clumpiness of either individual tree or total site CM layers. It is defined as a deviation from the tree/site CM mean:

$$S_k = \{\Sigma[(CM-CM_\mu)^3]\}/[(n-1)*s^3] \quad \text{eq. 7}$$

where CM_μ is the tree/site average CM, n is the number of layers in the tree/site canopy, and s is the standard deviation of the CM layers of the tree/site.

Topographic information was also taken into account for CBD remote sensing model development. Topographic saturation index (TSI) was used to account for stand-level average tree heights. TSI is given by:

$$TSI = \ln\alpha/\tan\beta \quad \text{eq. 8}$$

where α is the upslope drainage area for any given site and β is the slope of the site (Quinn, et al, 1995). These data were generated in ArcMap (ESRI, Redlands, CA) using digital elevation models (DEM) from Texas Natural Resources Information System (TNRIS).

These data were compiled in a Microsoft Excel spreadsheet and analyzed using StatsDirect. Comparisons were carried out using unpaired T-tests where data were normally distributed and Mann-Whitney analysis where data were neither normally distributed normally capable of being transformed to normal distributions. For multiple comparisons, data were analyzed with ANOVA where normal, and Kruskal-Wallis analysis where normality was not noted, nor achievable by transformation. Normality of data was assessed by Shapiro-Wilkes test for non-normality. Significance of results was ascertained using $\alpha=.05$ for all analyses.

Imagery from LANDSAT 7 ETM+ from July 2001 was utilized in an attempt to correlate field data with remotely sensed information. LANDSAT bands 3 (red) and 4 (near IR) were used to derive normalized difference vegetation index (NDVI) values for all pixels encompassing all plots measured in this study using GPS coordinates taken in the field (UTM, WGS 84). NDVI is calculated using Bands 3 and 4:

$$NDVI = (B4-B3)/(B4+B3) \qquad \text{eq. 9}$$

Spectral data were extracted in ERDAS Imagine (ESRI,) and compiled in Excel (Microsoft,). These data were analyzed in SPSS for significant correlation to field-measured CBD values. Multiple linear regression modeling was later used to derive a significant correlation between field data and LANDSAT 7 ETM+ data from March 2003 and September 1999.

Table 3. Comparison of canopy fuel parameters and value of skewness between BCP and BCNWR. All values given are mean ± standard deviation. The symbol * indicates significant differences exist among samples from the two refuges.

Parameter	BCP	BCNWR	*J. ashei* only	All
Sites sampled	32	42	7	74
Trees sampled	33	69	36	102
CBD (g/m^3)	26.04 ± 12.73*	20.73 ± 9.55*	28.44 ± 9.68	23.03 ± 11.27
Max CM (g/m^3)	81.53 ± 36.42	65.29 ± 43.86	96.39 ± 78.35	72.31 ± 41.34
TAF (g/m^2)	193.91 ± 67.64*	153.30 ± 60.32*	190.89 ± 80.72	170.86 ± 66.31
LAI (m^2/m^2)	2.69 ± 0.72	2.52 ± 0.67	2.303 ± 0.66	2.59 ± 0.69
Height (m)	8.47 ± 2.00	7.86 ± 2.09	6.86 ± 1.86	8.12 ± 2.06
CBH (m)	1.91 ± 1.17	2.17 ± 1.34	5.14 ± 1.77	2.05 ± 1.27
Canopy Length (m)	6.56 ± 1.97	5.69 ± 1.77	1.71 ± 0.95	6.07 ± 1.90
Skewness	0.925 ± 0.674*	0.661 ± 0.601*	N/A	0.746 ± 0.635

Independent T-test analysis using the equal variance assumption showed statistically significant differences in mean CBD values (p=.022), indicating higher mean CBD values for sites measured on BCP. Also TAF values on BCP were significantly higher than TAF values on BCNWR (p=.0017). Individual tree CM skewness data were also significantly higher (p=.0244) skewness values for trees measured on BCP compared to those measured on BCNWR. Due to low sample size, pure *J. ashei* stands were not analyzed in statistical comparisons of fuel parameters.

Significant differences existed between LMA values among species as found by pairwise comparison utilizing ANOVA and Tukey's HSD analysis. These differences were ranked where 1 is the highest magnitude of LMA and 3 is lowest level of LMA. *J. ashei* leaves yielded significantly higher LMA values then *Q. fusiformis*, which yielded significantly higher values of LMA than *Q. sinuata* and *Q. buckleyi*. *Q. buckleyi* and *Q.*

Table 4. Comparison of tree fuel parameters and value of skewness by species. All data given are mean ± standard deviation where appropriate. The symbol * indicates that significant differences exist between this value and at least one of the other species.

Species	*J. ashei*	*Q. buckleyi*	*Q. fusiformis*	*Q. sinuata*	All
Trees sampled	26	33	21	18	102
Leaf samples	169	257	140	115	681
LMA (g/m^2)	83.1 ± 11.1*	38.7 ± 7.3*	73.6 ± 11.7*	47.2 ± 11.4*	57.9 ± 21.6
LMA ranking	1	3	2	3	N/A
CM (g/m^3)	29.39± 10.45*	16.38 ± 6.14*	25.88 ± 8.93*	20.18 ± 10.29*	22.10 ± 10.30
CM ranking	1	3	1,2	2,3	N/A
CM Skewness	0.352 ± 0.562	0.688 ± 0.723	0.872 ± 0.667	0.901 ± 0.456	0.746 ± 0.635

sinuata LMA values did not significantly differ in LMA magnitude. Pairwise comparison utilizing Kruskal-Wallis analysis showed significant differences in the distributions of tree CM distributions by species. *J. ashei* trees tend to have highest CM layers, followed by *Q. fusiformis*, then *Q. sinuata*, and finally, *Q. buckleyi*. 95% confidence intervals did overlap among species as follows: *J. ashei* overlaps with *Q. fusiformis*, *Q. fusiformis* overlaps with both *J. ashei* and *Q. sinuata*, and *Q. sinuata* overlaps with *Q. buckleyi*. These overlaps are signified where more than one numeral is given in the row labeled CM ranking. Multiple numerals on one species indicate that that species' data overlapped two levels of ranking in the Kruskal-Wallis analysis. No significant differences in CM skewness were noted between species in this analysis.

Sites with *J. ashei* present tend to have significantly higher (p=.0049) values of TAF. Sites with *Q. fusiformis* tended to have higher Max CM values than sites without

Q. fusiformis (lower side p=.0017). Analysis also shows that sites with *Q. fusiformis* present.

Table 5. Comparison of sites for canopy fuel structure with respect to presence/absence of four major species. Values shown are mean ± standard deviation. *Indicates significant differences exist between sites where species present compared to those where species is absent.

Fuel	*J. ashei*		*Q. buckleyi*		*Q. fusiformis*		*Q. sinuata*	
measure	Present	Absent	Present	Absent	Present	Absent	Present	Absent
CBD (g/m^3)	24.08± 11.45	18.15± 6.61	17.62± 6.49*	26.04± 9.35*	25.12± 8.84	21.16± 9.14	24.29± 10.28	25.52± 30.56
Max CM (g/m^3)	74.05± 43.42	64.88± 31.10	54.80± 29.66*	86.41± 44.26*	86.21± 32.69*	66.81± 43.36*	74.54± 37.83	71.60± 42.71
TAF (g/m^2)	178.90± 69.83*	136.38± 31.33*	143.47± 47.33*	192.90± 71.52*	191.23± 55.25*	162.79± 69.02*	182.30± 83.55	167.18± 60.18
LAI (m^2/m^2)	2.55± 0.70	2.77± 0.66	2.71± 0.67	2.49± 0.70	2.33± 0.59	2.70± 0.71	2.76± 0.71	2.54± 0.68

tend to have higher TAF values than sites without *Q. fusiformis* (p=.002). The results of an unpaired T-test support the conclusion (p<.0001) that sites with *Q. buckleyi* present have significantly lower CBD values than sites without this species. Unpaired T-test results further indicate that Max CM values in sites with *Q. buckleyi* are significantly lower (p<.0001) than those values in sites without *Q. buckleyi* present. Mann-Whitney analysis results (p=.0001) indicate that sites with *Q. buckleyi* also tend to have lower values of TAF than sites without this species.

A multiple linear regression modeling approach was used to derive a model suitable for spectral modeling of the CBD of BCP and BCNWR. This model utilizes data from multiple datasets. The best fit model (c) was used to predict ln(CBDMax). It is

comprised of Landsat bands 3, 4, and 5 from March 2003, band 3 from September 1999, and TSI. This model is significant (p=.004), explains variation in ln(CBDMax)

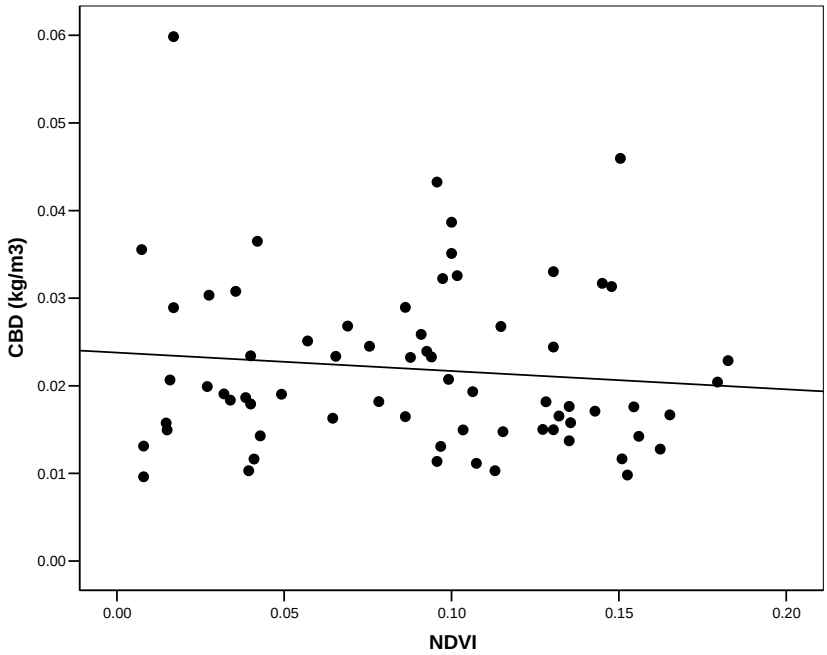

Figure 5. CBD does not correlate with NDVI. Linear regression modeling was used to compare CBD values and NDVI values from LANDSAT 7 ETM+ July 2001 imagery. The correlation was not significant (r^2=.0457). Following partitioning of the NDVI values by topographic zones based on the TSI values also showed no correlation.

Table 6. CBD multiple linear regression model. Ln (CBDMax) was estimated with this model derived from digital number values from multiple LANDSAT 7 ETM+ images and TSI values created in ArcMap from Texas DEM's.

Predictors	R	R Square	Adjusted R Square	Std. Error of the Estimate	Durbin-Watson
MB4, TSI, SB3, MB3, MB5	0.632	0.399	0.308	0.41885	1.278

around 30% accurately (adjusted r^2=.308), and does not have excessive auto-correlation (Durbin-Watson coefficient=1.278). The complete model is as follows:

ln (CBDMax) = (.045 MB4)+(.089MB3)+(.060SB3)-(.065MB5)-(.056TSI)-7.56 eq.10

Table 7. ANOVA results for multiple linear regression model.

Model	Sum of Squares	df	Mean Square	F	Significance
Regression	3.849	5	0.770	4.388	0.004
Residual	5.789	33	0.175		
Total	9.639	38			

Where CBDMax is given in kg/m^3, M relates to imagery taken from March 2003, S relates to imagery taken September 1999, B3 is band 3 digital number, B4 is band 4 digital number, B5 is band 5 digital number, and TSI is topographic saturation index.

Discussion

Analysis of the data between the two refuges showed that mean CBD and TAF values are significantly higher on BCP than BCNWR (Table 3). The result indicates heavier total fuel loadings on canopies due to varying ecological factors. Differences in disturbance regimes are possible due to ex-urbanization, a history of thinning by humans, and greater topographic relief on BCP that can affect wind-derived pruning and extent of fires on BCP. The BCP woodlands contain few open spaces and grasslands adjacent to BCP woodlands that increase wind damage on trees. On the BCWNR, fire management has encouraged grasslands through elimination of emergent woody growth. Another possible explanation may be canopies reaching mature states at BCP faster than at BCNWR. This could be due to site productivity advantages on BCP, based on BCP's lower elevations and higher site soil water availabilities. Alternatively, enhanced crown growth on BCP may be due to the relationship between limited spatial extent of fires and fire behavior on BCP. Smaller areas of contiguous fine fuels on BCP presumably result in smaller fires with less reaction intensity, shorter flame lengths, and less crown fire. On

BCNWR, active prescribed burning may result in lower crown fuel levels in these woodlands compared to those on BCP due to the effects of micro-climate alteration that occur post fire when edges have been disturbed. Large crown fires on BCNWR are not common but prescribed burning operations frequently result in torching and passive crowning at grassland-woodland interfaces.

The difference in the distribution of foliage in canopies between BCNWR and BCP based analysis of skewness (Table 3) indicates that canopies on BCNWR are less clumpy than at BCP. This result coincides with differing TAF levels between the refuges and is likely due to the same causes: lower winds, higher productivity, and greater maturity. These results hold significance for fire management on these refuges as higher levels of fuel loading and clumpier canopies would tend to yield greater torching/crowning probability and intensity on BCP. This leads to less predictability of crown fire extent, reaction intensity, and frequency.

Differences among species in LMA (Table 4) are important because higher LMA values, such as in *J. ashei* and *Q. fusiformis*, can burn hotter due to higher biomass to surface area ratios. Mass-area ratios also give an indication of how fuels will resist burning (when well-watered) as well as how fast these can potentially desiccate under drought conditions. While the biomass available to be burned in *Q. buckleyi* and *Q. sinuata* canopies tends to be lower than that in the canopies of *J. ashei* and *Q. fusiformis*, the deciduous oak species will be dried more rapidly under drought conditions or with pre-frontal heat-drying in wildfires because of their lower mass/area ratios. Drying will occur more slowly in the higher LMA evergreen canopy species, though under dry conditions these fuels should yield more energy when burned. As conditions dry, both

canopy types can yield readily ignitable crown fuel conditions. Since no significant differences were noted in LAI where species presence/absence was taken into account (Table 5) it can be reasoned that CM layer differences among trees of different species (Table 4) are due to LMA differences where leaf area noted at each site for any species yields higher density for species with higher LMA.

Differences among sites in CBD on the basis of presence/absence of any one species are only significant in the case of *Q.buckleyi* (Table 5). Lower levels of CBD at sites where this species is present are likely due to a combination of *Q. buckleyi*'s frequent dominance of sites, coupled with its low LMA (Table 2) values. Physiologically, *Q. buckleyi* may have lower LMA values because its stomatal conductance values are higher than the other species examined here and it shuts down at less negative water potential levels (Sides, 2007). The result of this is a reduced risk of torching and crown fire initiation in sites where this tree is prevalent. Differences detected in Max CM layer where *Q. buckleyi* is present showed that sites where this tree is present tend to have lower maximum layer CM than those where it is absent. The result of this is lowered crown fire intensity when crowning occurs. Since most Max CM layers exist in the upper reaches of canopies, this result has little effect on crown fire initiation or torching, but does impact contiguity of fuel from one tree to the next. TAF levels are also significantly lower in sites that contain this species versus those not containing it. Based on the result that LAI values do not differ for sites with this species, TAF, CBD, and Max CM differences are all likely due to differences in LMA (Table 2). Lowered reaction intensities and less dense fuel layers in the upper reaches of *Q. buckleyi* canopies can yield slower moving crown fires with lower temperatures. Canopies where

this species is prevalent could slow or stop crown fire movement under certain conditions.

Max CM layer levels in canopies where *Q. fusiformis* is present are significantly higher than in those without this species (Table 5). This result is likely due to higher average LMA values (Table 2) in this species. This result indicates increased crown fire intensity and fuel contiguity in canopies where this species is prevalent. TAF values were also found to be significantly higher in sites containing *Q. fusiformis* than in those where it is absent. This result leads to a picture of these canopies where *Q. fusiformis* is dominant with some understory. Crown fire is likely here under certain conditions and it can carry rapidly and with high intensity.

The finding that *J. ashei* containing canopies have neither higher CBD, or Max CM (Table 3) is curious based on its higher LMA (Table 4). This finding is likely due to *J. ashei*'s lack of dominance in many of the canopies where it was found. Though it is a very common tree on both BCNWR and BCP, it is less frequently the dominant overstory species in locations where other species exist. In sites that are pure *J. ashei*, it is dominant and its fuel characteristics are considerably higher than those where other species are present. Its average CBD is 28.44g/m^3 and Max CM is 96.39g/m^3, both of which are much higher than average values from this study. Only 7 sites were measured where this is the only species present, thus these results were not considered in the analysis above, though the data for this type of stand (Table 3) should be used for fire behavior modelling where mono-cultural *J. ashei* stand conditions are known to exist. TAF values for sites that contain *J. ashei* were significantly higher than those not

containing this species. This further underscores the fuel density differences in this species and those which it co-exists.

Q. sinuata canopies do not significantly differ in fuel characteristics from other sites measured in this study. This means that fire behavior in this site will be similar to averages from across both refuges and should be modelled as such. This result is likely due to the frequency of which *Q. sinuata* is found as a sub-dominant or intermediate part of canopies at both BCP and BCNWR. It is important to note that short, shrubby, shinneries were not measure in this study as these constitute brushy fuel and thus have very different canopy fuel characteristics and crown fire behaviors from the mature, tall canopies this study was designed to examine.

Poor fit in all attempts (fig. 5, tables 6 and 7) to reconcile ground CBD data with spectral data from LANDSAT 7 ETM+ imagery implies that such a correlation does not exist. Theoretically, plant biomass density should correlate to spectral reflectance indices (Park and Deering, 1982) based on differential scattering of light spectra by foliar material. LANDSAT 7 band 3 is sensitive to reflectance from 0.63-0.69µm while band 4 is sensitive to reflectance from 0.75-0.90µm. Radiation in the spectrum of band 3 is absorbed by chlorophyll while that in band 4 is scattered by leaf surfaces. It is therefore likely that foliar biomass density measures, such as CBD, would inversely correlate to any spectral index built by the quotient of radiant energy absorbed by the sensor in Band 4 to that absorbed by band 3. Due to the method employed here, whereby LAI is measured at 1-m vertical intervals for a plot, LAI measurements encompass an expanding cone of measurement. This method, coupled with spatial heterogeneity of LAI, could lead to individual plot data that do not fully represent the pixel(s) in which the plot

occurs. Interannual variability may also be a source of error that results in a lack of correlation between field and spectral data as the field data were taken summer 2006 and summer 2007, several years after the LANDSAT data (July 2001). Finally, species differences in leaf coloration and density (LMA) may reflect sunlight differently at a given density, thus making remote measurement of mixed species stands untenable with LANDSAT 7 ETM+ data. Hyperspectral information across a time series may be necessary to yield significant relationships between field data and remotely sensed canopy reflectance information. The multiple linear regression approach shown here (fig. 2) was used to create a data layer to represent heterogeneous canopy structures for the study area. This is a valid, though low fidelity and over-fit approach to the problem of CBD mapping.

CBD is a complex stand parameter. It involves leaf mass, leaf area, and tree height. Integrating these factors at a stand level based on field measurements results in remote sensing complexities that are difficult to account for. CBD maximum layers relate to spectral reflectance and topographic data based on physical principles. First, May imagery relates to peak growth and thus to highest levels of LAI and moisture content in most growing seasons. Since measurements from the first sampling season (2006) were made in abnormally dry conditions and those made in the second sampling season, abnormally wet, interannual variability in leaf area and turgor pressure was covered. Thus the canopy measurements made in this study amount to generalizations of leaf area and moisture across a gradient of moisture conditions. Bands 3 and 4 from May imagery account for the differential scattering of light in these spectra by leaves that correlates to LAI. Leaf thickness is accounted for by band 5, which normally relates to

moisture content of foliar matter. Late season imagery, (September) also enhanced modeling efforts when band 3 was incorporated into the model. This is due to the same physical variables that make band 3 a good candidate for prediction of foliar matter in early season imagery. TSI correlates to CBD by taking into account generalities in stand-level average tree height. Well watered, deep soil sites generally produce trees that are taller than less well watered, shallow soil areas. Together these factors approximate prediction of CBD.

Conclusions

Canopy fuel conditions can differ significantly across sites with histories of differing land use, differing disturbance regimes, and/or site productivities. BCP lands tend to have higher fuel loads and higher degrees of crown fuel clumping than those of BCNWR, yielding less predictable results in fire behavior analysis and crown fire prediction. Inherent in this are the effects on fuel structure associated with stand age and time since disturbance. Important disturbances in this regard can include land clearing, posting, wind shear, and crown fire. These set back crown development and lead to overall lower fuel loading and higher fidelity crown fire prediction and behavior modeling.

Species-type can lead differences in crown fuel loadings. Non-deciduous, high LMA species sampled in this study yielded higher crown fuel loadings and densities, which can lead to more torching, higher crown fire extents, and greater fire effects (reaction intensity and heat output). Sites on BCP and BCNWR should be assessed for species make-up to achieve highest predictive accuracy in fire behavior modeling. Sites should be organized into pure *J. ashei*, mixed non-deciduous, mixed deciduous, and pure

deciduous stand types to achieve highest levels of predictive ability in crown fire probability detection attempts.

CHAPTER FOUR

Comparison of FARSITE Fire Simulations Using Homogeneous and Heterogeneous Crown Fuel Layers

Abstract

Crown fuel densities were estimated using two approaches: remotely sensed CBD layer mapped from multiple linear regression modeling as a treatment variable, and average field measured CBD value layer mapping as a control variable. Both winter and summer fires were simulated using the same 20 ignition points and the same fuel and topographic layers. Outputs were compared and statistically significant differences noted between treatments. Total area of crowning was significantly higher ($p=.008$) with homogeneous, control CBD mapping, while active crown fires were only noted with heterogeneous CBD mapping. Differences between the two refuges utilized in the study were also noted, based primarily in differences in spatial extent of fires and availability of large tracts of unbroken fine fuels on BCNWR, compared to BCP. Summer and winter fires were also compared where summer burns showed significantly higher levels of spatial fire extent, area of crown fire, reaction intensity, and heat per unit area in some or all treatments.

Introduction

FARSITE (Finney, 1994) is a commonly used, readily available fire simulation engine based on Rothermel's (1972) surface fuel spread model. It requires several data layers including: surface fuel model, slope, aspect, and elevation. Also required are wind

and weather input parameters or files. Technicians frequently utilize this simulator to plan prescribed burns and assist with planning for wildland fire suppression efforts. Anderson's (1982) 13 fuel models are available in FARSITE, and are the most commonly used surface fuel model inputs. These models may oversimplify fuel parameters.

Crown fuels are not necessary inputs for FARSITE fire behavior modeling. Since crown fuel averages are present in Anderson (1982) fuel layering, these data are accounted for at a general level. This is a misleading situation however, since fuel averages do not account for spatial heterogeneity, mixed species stands, or fuel types that are not adequately treated in current fuels modeling. Custom crown fuel modeling is necessary to enhance fire behavior predictability in future fire and land management efforts.

The *J. ashei* dominated, mixed oak woodlands of the Balcones region are not adequately treated by current fuel models. Most fire managers make judgment calls when assigning this landscape to an Anderson fuel model. This can lead to inconsistencies and poor predictive accuracy of fire behavior modeling. Enhancing the ability of land and fire management officers to assign fuel characteristics to this landscape is a necessary next step to managing this already underburned landscape. Further, prescribed crown fire is likely to be a necessary step in the near future to promote oak regeneration at the expense of the dominant *J. ashei*. To predict accurately what areas are susceptible to continuous crowning under burn conditions, fire behavior simulation models, such as FARSITE, are the best tool currently widely available.

Materials and Methods

Fuels data layers were by using spectral signatures to assign a custom fuel classification to each pixel in the landscape using LANDSAT 7 ETM+ datasets (White and Sides, *unpublished data*). Custom fuel models were created from field data taken summer 2007. Ground layer fuels data were taken by utilizing a line intercept method known as Brown's fuel transect (Brown, 1986). These data were geo-located with handheld GPS units (Garmin, Olathe, KS) and total fuel loadings calculated and distributed in fuel size classes.

Topographic layers (elevation, aspect, and slope) were prepared using downloadable DEM data from Texas Natural Resources Information System (TNRIS). These DEM's were processed in ERDAS Imagine (Leica Geosystems, St. Gallen, Switzerland). Data layers were diced to the same size to cover the entire area of both refuges. These were then input to FARSITE and a landscape file was generated. FARSITE is available as a free download from http://www.fire.org.

Maximum 1m layer CBD mapping was achieved with a multiple linear approach outlined above. This layer was fit over all fuel models considered forested. As a control, average maximum 1m layer CBD values of 0.07kg/m^3 were used in simulations identical to those used with the treatment CBD layer. Crown cover was a constant 80% while crown base height (CBH) was set at the average value taken from field data (2.1m). Canopy height in wooded areas was set to a constant 8m (average from field data). Though variation in canopy cover, CBH, and canopy height were noted in field data collection, these variables were kept constant to test the effects of heterogeneous crown fuel density mapping against a control.

Weather and wind files for the behavior simulations were created by Ms. Mary Sides and were based on worse-case scenarios of known fire weather in the area. Summer fires were initiated on July 4 and winter fires January 4 with a one day drying pre-drying period and allowed to run for 24 hours. No suppression methods were simulated. Fire behavior characteristics were collected as outputs from FARSITE and analyzed in ArcMap (ESRI, Redlands, CA). FARSITE outputs two different types of crown fire: active and passive. These were segregated in data collection and crown area was calculated as the sum of both active and passive crown fire extent, while active crown area was further analyzed as a separate entity. These data were then compiled into tables, checked for normality of distribution using Kolmogorov-Smirnov analysis and statistically compared using paired or independent Student's T-tests in SPSS (SPSS, Inc., Chicago, IL).

Results

Table 8. Comparison of fire behavior parameters between modeled and average CBD inputs in summer scenarios. Values shown are mean ± standard deviation. The symbol* indicates significant differences exist.

Refuge	Fire Area (Ha)	Crown Area (Ha)	Active Crown Area (Ha)	Crown Ratio	Reaction Intensity (kW/m)	Rate of Spread (m/s)	Heat per unit Area (kJ/m^2)
Modeled	2531±2109	111.9±94.2*	3.48±3.71*	0.041±0.011*	294±19	3.06±1.28	3767±292
Average	2532±2023	441.7±531.3*	None*	0.113±0.059*	294±19	3.06±1.28	3767±292

Table 9. Comparison of fire behavior parameters between modeled and average CBD inputs in winter scenarios. Values shown are mean ± standard deviation. The symbol* indicates significant differences exist.

Refuge	Fire Area (Ha)	Crown Area (Ha)	Active Crown Area (Ha)	Crown Ratio	Reaction Intensity (kW/m)	Rate of Spread (m/s)	Heat per unit Area (kJ/m^2)
Modeled	1444±1050	61.1±50.0	3.54±3.03*	0.038±0.009	268±24	3.37±1.38	3539±344
Average	1444±1050	61.1±50.0	None*	0.038±0.009	281±57	3.37±1.38	3539±344

Mean crown fire area for summer burn simulations was significantly higher (p=.008) for fires simulated with homogeneous CBD mapping than simulations with heterogeneous CBD mapping. Active crown fire areas were significantly higher for fires with heterogeneous canopy mapping in both summer and winter (p<.001) burn scenarios as no active crown fire occurred with homogeneous CBD map layers. Ratio of crown fire activity to total fire area was significantly higher (p<.001) for fires simulated using homogeneous average CBD map layers in summer burn scenarios.

In both control and treatment simulations, mean fire areas were significantly larger in summer burns (p=.001). In crown fire area, summer burns showed significantly greater crown fire extent with heterogeneous (p<.001) and homogeneous (p=.002) canopy layer treatments than did winter burns. Reaction intensities with heterogeneous canopy mapping were significantly higher (p<.001) in summer burns than winter burns. Summer burns also showed significantly higher (p<.001) heat per unit area compared to winter burns when both landscape sets were modeled with heterogeneous and homogeneous canopies.

Table 10. Comparison of summer scenario fire behavior parameters between refuges with modeled CBD. Values shown are mean ± standard deviation. The symbol* indicates significant differences exist.

Refuge	Fire Area (Ha)	Crown Area (Ha)	Active Crown Area (Ha)	Crown Ratio	Reaction Intensity (kW/m)	Rate of Spread (m/s)	Heat per unit Area (kJ/m^2)
BCP	1576±868*	64.8±34.5	2.93±3.08	0.039±0.012	287±16	2.53±1.09	3688±315
BCNWR	3485±2413*	158.9±112.4	4.02±4.35	0.043±0.010	300±21	3.59±1.29	3846±259

BCP and BCNWR summer fire simulations resulted in significantly higher spatial extent on BCNWR lands with treatment (p=.019) and control (p=.019) CBD layers. In winter burns, significantly greater spatial extent was noted in treatment (p=.018) and

Table11. Comparison of summer scenario fire behavior parameters between refuges with average CBD. Values shown are mean ± standard deviation. The symbol* indicates significant differences exist.

Refuge	Fire Area (Ha)	Crown Area (Ha)	Active Crown Area (Ha)	Crown Ratio	Reaction Intensity (kW/m)	Rate of Spread (m/s)	Heat per unit Area (kJ/m^2)
BCP	1576±868*	157.3±184.8	None	0.08±0.05*	287±16	2.53±1.09	3688±315
BCNWR	3489±2419*	726.1±618.1	None	0.15±0.04*	300±21	3.59±1.29	3846±259

Table 12. Comparison of winter scenario fire behavior parameters between refuges with modeled CBD. Values shown are mean ± standard deviation. The symbol* indicates significant differences exist.

Refuge	Fire Area (Ha)	Crown Area (Ha)	Active Crown Area (Ha)	Crown Ratio	Reaction Intensity (kW/m)	Rate of Spread (m/s)	Heat per unit Area (kJ/m^2)
BCP	956±716*	36.8±27.0	2.47±2.00	0.04±0.01	264±18	2.74±0.88*	3428±263
BCNWR	1931±1134*	85.4±56.9	4.61±3.59	0.04±0.01	272±30	4.00±1.53*	3651±391

Table 13. Comparison of winter scenario fire behavior parameters between refuges with average CBD. Values shown are mean ± standard deviation. The symbol* indicates significant differences exist.

Refuge	Fire Area (Ha)	Crown Area (Ha)	Active Crown Area (Ha)	Crown Ratio	Reaction Intensity (kW/m)	Rate of Spread (m/s)	Heat per unit Area (kJ/m^2)
BCP	956±716*	36.8±27.0	None	0.04±0.01	289±76	2.74±0.88*	3428±263
BCNWR	1931±1134*	85.4±56.9	None	0.04±0.01	272±30	4.00±1.53*	3651±391

control (p=.018) scenarios. In control CBD layered summer burn scenarios significantly higher (p=.002) ratios of crown fire to surface fire spatial extents were evident on BCNWR. Winter simulations resulted in significant (p=.020) differences in mean rates of spread in control and treatment CBD layered scenarios.

Table 14. Pixel CBD parameters for type 3 crowned pixels in simulated ignition 12.

Sample number	Minimum (g/m^3)	Maximum (g/m^3)	Mean (g/m^3)	Standard Deviation (g/m^3)
30	121	400	243	94

Discussion

Control and treatment variable CBD layers resulted in differences in fire behavior in some simulations. Crown fire area was higher with control CBD layering (Tables 8 and 9). This indicates that spatial heterogeneity is an important factor in canopy fire braking. Less dense areas can reduce spread from passive crowning. Furthermore, highly variable crown fuels lead to variable crown fire behaviors. Active crowning did not occur in fires simulated with average value CBD layers. This indicates that crown fuel heterogeneity acts in both directions: increasing high intensity active crown fire under dense fuel conditions and stopping crown fire under low fuel densities.

Large tracts of contiguous, homogeneous fuels can create widespread crown fire activity. Based on the no difference result in wintertime simulations (Table 8), deciduous canopy mass dynamics appear to be the defining factor in these differences. This is further validated when considering the highly homogeneous nature of *J. ashei* canopies. Furthermore, based on the heterogeneity of both control and treatment canopies encountered in the winter scenarios, heterogeneity in CBD plays a major role in diminishing spatial extent of crown fire activity.

Crown fire ratios were significantly larger in summer fires on BCNWR than BCP under homogeneous crown fuel simulations (Table 11). This result underscores the importance spatially extensive burns can have on crown fire behavior. Larger fires result in higher intensity fires and longer flamelengths, thus greater probabilities of crown fire as well as more intense crown fires, which result in higher fire movement inertia. Spatially extensive fires result in greater proportions of crown fire, particularly under fire-promoting weather conditions and homogeneous crown fuels.

Differences in rates of spread of fire fronts between the two refuges in winter burns (Tables 12 and 13) underscore the subtle differences in fire ecology between the two. BCNWR has larger tracts of unbroken fine fuel, and therefore fires can reach near peak levels of fire energy allowed by meteorological conditions. This can result in higher energy fires particularly at the downwind grassland-woodland boundary. Such an occurrence increases the likelihood and intensity level of crown fire. Though no statistical difference was noted in rate of spread in summer burns, the ratio of crown fire area to total burned area were significantly different in average CBD layer control burns (Tables 10 and 11). This indicates that fire energy can be impacted by spatial fire extent. Larger tracts of fine fuels result in higher levels of fire behavior, though the differences may not always be statistically significant when so many varied fires are examined.

In FARSITE, the types of crown fire, passive and active, are determined by threshold levels of crown fire spread rate that are inversely proportional to CBD (Finney, 1998). Thus, lower CBD values raise the threshold of active crown fire spread and decrease the likelihood that surface fire reaction intensity levels will achieve values large enough to propagate such an active crown fire. This underscores the utility of heterogeneous CBD modeling when attempting to predict fire behavior danger areas for prescribed burning or fire risk assessment. Thirty mapped CBD points randomly selected showed that all exceeded the average CBD value utilized in homogeneous simulations. Mean value (0.243 kg/m^3) of these randomly selected points were more than three times as larger than the average values (0.070 kg/m^3) with the highest value mapped (0.400 kg/m^3) (Table 12). The range of CBD in these woodlands are higher than values for

woodlands and forests from other U.S. regions, making the need for site specific CBD important for future fire simulation work in these ecosystems.

Differences in winter and summer simulation fire behavior, underscore ecological implications of the season in which a crown fire occurs. Spatial extent of crown fuels is diminished and patchier in winter burns, particularly in areas with large deciduous tree components. This is evidenced by the larger fire extents in these simulations in summer burns with all treatments. Winter burns may be ideal for management of aggressive, evergreen species such as *J. ashei*. Prescribed crown fires would be easier to control and less damaging to deciduous trees in these burns. Elevated reaction intensities and heat per unit area in summer burns would cause greater fire danger in urban-interface areas and would result in more extensive habitat destruction. These findings imply that spatial heterogeneous crown fuels result in lower fire energy and can be an aid in the removal of evergreens in winter burns.

In the simulations tested here the heterogeneous CBD provided active crown fires that did not occur with homogenous CBD input layers (Tables 8 and 9). This is related to a threshold value of CBD necessary for contiguity estimates in simulation calculations to result in this type of fire (Finney, 1998). Threshold values that define crown fire type in FARSITE are based on the equation:

$$RAC = 3.0/CBD \qquad \text{eq. 11}$$

where RAC is the rate of active crown fire spread and the constant 3.0 was determined empirically (Alexander, 1988). The maximum mapped CBD values was 0.400 kg/m^3 in canopy based on the multiple linear regression approach. Since use of a single average value (0.070kg/m^3) resulted in no active crowning, it can be assumed that initiation of

active crown fires requires higher CBD values. The lowest CBD value to simulate an active crown fire utilizing the heterogeneous CBD values was 0.121 kg/m^3. This is likely to be near the threshold value of CBD necessary to initiate active crowning event in FARSITE under the weather and fuel conditions simulated here. Summer fire simulation based on ignition point 12 with heterogeneous crown fuels mapping was intensively analyzed to determine which pixels experience the highest intensity (level 3) crown fire behavior.

Conclusion

Results of these analyses show that extensive mapping of CBD is necessary to predict extreme fire situations, most notably extensive continuous crown fire behavior. This is the most dangerous fire situation for suppression teams, citizens in adjacent areas, and wildlife. Furthermore, when a prescribed crown fire is required to shift relative species abundances from junipers to oaks in this landscape, pre-existing knowledge of likely crown fire behavior could prove invaluable to land managers.

Woodland fires area sensitive to adjacencies, particularly proximity to large tracts of fine fuels that can propagate higher intensity fires. In fires that have smaller spatial extents, the possibility of active crown fire initiation is limited by the lack of energetic fire behavior that can occur. Fires need to build energetic momentum to develop crowning potential.

CHAPTER FIVE

Conclusion

An understanding of foliar traits at multiple scales is important for modeling stand and ecosystem level processes. Utility in modeling and land management projections is dependent on knowledge of interactions between leaf structural and nutritional traits and the implications these have for stand and ecosystem level characteristics.

Leaf morphology has been shown to relate to species' leaf longevity, as well as ambient light conditions. Further, a model has been proposed to encompass the interactions between leaves, radiation, and water to explain expansion and thickening of leaf material. This model implies that leaf expansion is affected by physical forces that are similar across phylogenies, thus the mechanism is evolutionarily conserved. Leaf nutrients nitrogen and phosphorus have been shown to also be related to light environment. Leaf N was shown to differ on a functional group basis, related to leaf longevity patterns. Leaf stoichiometry also has been implicated as an adaptive factor that affects alteration of a plant's immediate environment possibly enhancing its competitive advantages, based on life history characteristics of the species involved.

Structural traits of canopies have been shown to relate to the presence or absence of species in the study area. This couples canopy fuel parameters directly to leaf morphology characteristics of the species involved. Further, differences in canopy fuels are shown to exist between the two highly similar refuge sites of the study area. This connects land use history characteristics and disturbance regime differences to

differences in stand level canopy characteristics. Fuel dynamics altered by disturbance regime differences can serve as feedbacks that cause landscape mosaics to develop.

Such spatial heterogeneity can further modulate disturbance regimes as crown fuel variability was shown to result in crown fire occurrences that were less frequent and extensive, though often more destructive. Seasonal patchiness in crown fuels such as that in deciduous canopies in wintertime can also serve to decrease crown fire extent.

Disturbance patterns are shown here to be highly sensitive to biogeographical factors, such as adjacency to large tracts of fine fuels and topographic fire brakes. Furthermore, aspect is an important determinant of species composition in this and many ecosystems, thus introducing spatial heterogeneity in crown fuels. This underscores the importance of understanding biogeographical interactions with disturbance patterns.

Ecosystem feedbacks are important to understanding overall system dynamics at all levels. However, enhancing the knowledge of interactions between these scales is a next step to productive modeling, land management, and advancing the science of ecology.

REFERENCES

Anderson, H.E. 1982. Aids to determining fuel models for estimating fire behavior. USDA Forest Service General Technical Report. INT-122, 22p.

Alexander, M.E. 1988. Help with making crown fire hazard assessments. In: Fischer, W.C. and S.F. Arno (compilers), Protecting people and homes from wildfire in the Interior West. USDA For. Serv. Gen. Tech. Rep. INT-251. pp. 147-156.

Austin, A.T., Yadjian, L, Stark, J.M., Belnap, J., Porporato, A., Norton, U., Ravetta, D.A., and Schaeffer, S.M. 2004. Water pulses and biogeochemical cycles in arid and semiarid ecosystems. Oecologia 141:221-235.

Brown, J.K., and Bevins, C.D. 1986. Surface fuel loadings and predict fire behavior for vegetation types in the northern Rocky Mountains. USDA For. Res. Note. INT-358.

Carey, J.H. 1992. Quercus stellata. In: Fire Effects Information System, [Online]. U.S. Department of Agriculture, Forest Service, Rocky Mountain Research Station, Fire Sciences Laboratory (Producer). Available: http://www.fs.fed.us/database/feis/ [2008, September 5].

Carey, J.H. 1992. Quercus virginiana. In: Fire Effects Information System, [Online]. U.S. Department of Agriculture, Forest Service, Rocky Mountain Research Station, Fire Sciences Laboratory (Producer). Available: http://www.fs.fed.us/database/feis/ [2008, August 6].

Dickinson, J., Robinson, A., Harrod, R., Gessler, P., and Smith, A. 2007. Modification of Van Wagner's canopy fire propagation model. USDA Forest Service Proceedings, RMRS-P-46CD, pp.83-96.

Ellsworth, D.S., and Reich, P.B. 1996. Photosynthesis and leaf nitrogen in five Amazonian tree species during early secondary succession. Ecology 77:581-594.

Finney, M.A. 1994. Modelling the spread and behavior of prescribed natural fires. Proc. 12th Conf. Fire and Forest Meteorology, pp. 138-143.

Finney, M.A. 1998. FARSITE: Fire area simulator – model development and evaluation. Res. Pap. RMRS-RP-4. Ogden, UT: U.S. Dept. of Agriculture, Forest Service, Rocky Mountain Research Station. 47 pp.

Green, D.S., Erickson, J.E., and Kruger, E.L. 2003. Foliar morphology and canopy nitrogen as predictors of light-use efficiency in terrestrial vegetation. Agricultural and Forest Meteorology 115:163-171.

Harley, P.C., Thomas, R.B., Reynolds, J.F., and Strain, B.R. 1992. Modelling photosynthesis of cotton grown in elevated CO_2. Plant, Cell, and the Environment 15:271-282.

Kazda, M., Salzer, J., and Reiter, I. 2000. Photosynthetic capacity in relation to nitrogen in the canopy of a *Quercus robur*, *Fraxinus angustifolia*, and *Tillia cordata* floodplain forest. Tree Physiology 20: 1029-1037.

Keane, R.E., Reinhardt, E.D., Scott, J., Gray, K., and Reardon, J. 2005. Estimating forest canopy bulk density using six indirect methods. Canadian Journal of Forestry Research 35:724-739.

Kirschbaum, M.U.F., King, D.A., Comins, H.N., McMurtrie, R.E., Medlyn, B.E., Pongracic, S., Murty, D., Keith, H., Raison, R.J., Khanna, P.K., and Sheriff, D.W. 1994. Modelling forest response to increasing CO_2 concentration under nutrient-limited conditions. Plant, Cell, and Environment 17:1081-1099.

Kleinbaum, D.G., Kupper, L., and Muller, K.E. 1988. Applied regression analysis and other multivariable methods 2nd Ed. PWS-Kent Publishing Co. Boston, MA. 718pp.

Meir, P., Grace, J., and Miranda, A.C. 2001. Leaf respiration in two tropical rainforests: constraints on physiology by phosphorus, nitrogen and temperature. Functional Ecology 15:378-387.

Monk, J. Sclerophylly in Quercus virginiana. 1987 Mill, Castanea, 52:256-261.

Myers, B.J. 1988. Water stress integral- a link between short-term stress and long-term growth. Tree Physiology 4:315-323.

Niinemets, U. 1999. Research review: components of leaf dry mass per area-thickness and density- alter leaf photosynthetic capacity in reverse directions in woody plants. New Phytologist 144:35-47.

Park, J.K., and Deering, D.W. 1982. Simple radiative transfer model for relationships between canopy biomass and reflectance. Applied Optics 21:303-309.

Pastor, J., Aber, J.D., McClaugherty, C.A., and Melillo, J.M. 1984. Aboveground production and N and P cycling along a nitrogen mineralization gradient on Blackhawk Island, Wisconsin. Ecology 65:256-268.

Pastor, J., and Post, W.M. 1986. Influence of climate, soil moisture, and succession on forest carbon and nitrogen cycles. Biogeochemistry 2:3-27.

Quinn, P.F., Beven, K.J. and Lamb, R. 1995. The ln(α/tanβ) index: how to calculate it and how to use it within the TOPMODEL framework. Hydrological Processes 9:161-182.

Rothermel, R.C. 1972. A mathematical model for predicting fire spread in wildland fuels. Res. Pap. INT-115. Ogden, UT: U.S. Dept. of Agriculture, Forest Service, Intermountain Forest and Range Experiment Station. 161 pp.

Sides, M. 2007. Personal communication.

Specht, R.L., and Specht, A. 1989. Canopy structure in *Eucalyptus*-dominated communities in Australia along climatic gradients. Oecologia Plantarum 10:191-213.

Sullivan, J. 1993. Juniperus ashei. In: Fire Effects Information System, [Online]. U.S. Department of Agriculture, Forest Service, Rocky Mountain Research Station, Fire Sciences Laboratory (Producer). Available: http://www.fs.fed.us/database/feis/ [2008, July 28].

Sullivan, J. 1993. Quercus shumardii. In: Fire Effects Information System, [Online]. U.S. Department of Agriculture, Forest Service, Rocky Mountain Research Station, Fire Sciences Laboratory (Producer). Available: http://www.fs.fed.us/database/feis/ [2008, September 5].

Takashima, T., Hikosaka, K., and Hirose, T. 2004. Photosynthesis or persistence: nitrogen allocation in leaves of evergreen and deciduous *Quercus* species. Plant, Cell, and Environment 27:1047-1054.

Turner, B.L., and Haygarth, P.M. 2001. Phosphorus solubilization in re-wetted soils. Nature 411:258.

Van Wagner, C.E. 1977. Conditions for the start and spread of crown fire. Canadian Journal of Forestry Research 7:23-34.

White, J.D., and Scott, N.A. 2006. Specific leaf area and nitrogen distribution in New Zealand forests: species independently respond to intercepted light. Forest Ecology and Management 226:319-329.